Review TRENDS in Biochemical Sciences Vol.32 No.9

The ribosome in focus: new structures bring new insights

Andrei Korostelev and Harry F. Noller

Center for Molecular Biology of RNA and Department of Molecular, Cell and Developmental Biology, University of California, Santa Cruz, 1156 High Street, Santa Cruz, CA 95064, USA

Recent all-atom crystal structures of 70S ribosome functional complexes provide a detailed description of how the ribosome interacts with its mRNA and tRNA substrates. The structures support the view that the fundamental steps of translation are based on RNA–RNA interactions, which in some cases underwent further refinement as a result of having recruited proteins. The structural basis of the discrimination of cognate tRNA, the high affinity for tRNA in the peptidyl-tRNA site, the structure of the peptidyl transferase catalytic center, the specificity of the exit site for deacylated tRNA and other functional properties of the ribosome are now explained, confirmed or visualized for the first time in complexes containing full-length tRNAs and defined mRNAs. Clues to the structural dynamics of translation are suggested by conformational changes that occur in both tRNA and the ribosome upon complex formation.

The ribosome in detail

The ribosome is a ribonucleoprotein complex that is responsible for protein synthesis in all living cells. Bacterial and archaeal ribosomes have a molecular weight of ~2.5 MDa, of which ~60% is RNA and 40% is protein. For several decades, the large size and highly dynamic nature of this molecular machine have made it difficult to infer structural details except with indirect biochemical and genetic approaches. Cryo-EM reconstructions allow visualization of the ribosome in different functional states [1–3], but at resolutions that do not permit a description of the atomic details of its molecular interactions (further discussion of which is beyond the scope of this review). Advances in X-ray crystallography have led to dramatic progress in structural studies of the ribosome. In 2000, all-atom structures of the large (50S) and small (30S) subunits of archaeal and bacterial ribosomes were solved [4–6]. Visualization of the interactions of the oligonucleotide analogs of tRNA and mRNA with the isolated 50S and 30S subunits led to detailed proposals for the mechanism of the peptidyl transferase reaction [7] and the role of the ribosome in codon–anticodon recognition [8]. Because the ribosome can use only full-length tRNA to carry out protein synthesis, crystal structures of the complete 70S ribosome complexed with intact tRNAs were also studied [9]. At 5.5 Å resolution, the RNA and protein backbones of the *Thermus thermophilus* ribosome that had tRNAs bound in the classical aminoacyl (A), peptidyl (P) and exit (E) sites could be fitted to the electron-density map [10]. The model provided a general description of tRNA-ribosome and subunit–subunit interactions but, because of its low resolution, lacked details that could reveal the roles of particular atoms in ribosome function. In 2005, Schuwirth *et al.* [11] described two 3.5 Å structures of the vacant *E. coli* ribosome, which greatly improved our understanding of intraribosomal interactions and the conformational flexibility of the ribosome at the molecular level. The next step was taken a year later, when the first all-atom structures of the *T. thermophilus* ribosome complexed with tRNA and mRNA were reported [12–14] (Figure 1). It is worth emphasizing that, although these tRNA-containing complexes were crystallized in different crystal forms, their solved structures reflect similar conformations of the ribosome and its substrates (Figure 2a): the root–mean–square difference between phosphorus atoms of the ribosome-tRNA complexes [12–14] is only 1.7–2.0 Å for either subunit, whereas the differences between the vacant [11] and tRNA-bound ribosome [12] are 3.1 and 3.7 Å for the 50S and 30S subunits, respectively (Figure 2b). This

Glossary

Methylated nucleotide nomenclature: This describes the location(s) of the methyl moiety(s) in the RNA nucleotide.
In the article, the following are referred to:
m5C 5-methyl-cytosine
m^2_2G 2,2-dimethyl-guanine
m^3U 3-methyl-uracil
type I and type II A-minor interactions: Tertiary RNA interactions involving hydrogen bonding and close steric fit between adenosine and the minor-groove surface of a Watson-Crick base pair [24].
D stem and D loop: Named for the one or more 5,6-dihydrouridine residues (abbreviated 'D') that are found in one of the loops of tRNA.
T stem and T loop: Named for the conserved ribothymidine residue that is found in the T loop at position 54 in tRNA; the T stem is the double helical stem that forms the base of the T loop.
Elbow: The corner of the tRNA three-dimensional structure, which resembles an elbow.
Hoogsteen edge: The edge of an RNA base that would be located in the major groove if the base were in a Watson-Crick base pair in a double helix. So named because the N7 and N6 positions of adenine lie on this edge and are involved in forming 'Hoogsteen' tertiary base pairs with uracil in many RNA structures.
Shine-Dalgarno (SD) sequence: A nucleotide sequence in most bacterial and many archaeal (but not eukaryotic) mRNAs that is found upstream from the start codon. The correct start codon is positioned in the ribosome by base pairing between the S/D sequence and a conserved CCUCC sequence near the 3′ end of 16S rRNA.
Bridge B1b/B1c: Two of the dozen molecular bridges that connect the 30S and 50S ribosomal subunits.

Corresponding author: Noller, H.F. (harry@nuvolari.ucsc.edu).
Available online 30 August 2007.

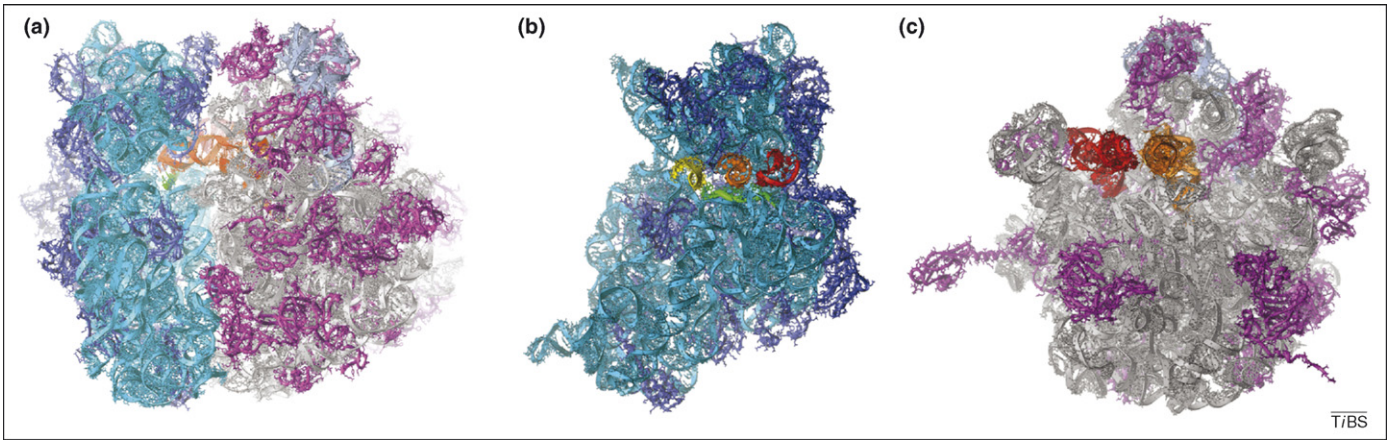

Figure 1. All-atom structure of a *T. thermophilus* 70S ribosome functional complex. **(a)** The whole 70S ribosome functional complex containing P- (orange) and E-site (red) tRNAs and mRNA (green) [13]. The complex is viewed from the side, as one looks down the path of the P to E sites between the large (50S) and small (30S) subunits. The large subunit 23S rRNA is shown in grey, 5S rRNA is shown in grey–blue and the large (L)-subunit proteins are shown in purple. The small-subunit rRNA (16S) is shown in cyan, and the small (S)-subunit proteins are shown in blue. **(b)** The 30S subunit of the 70S functional complex, viewed from the subunit interface. The ASL of A-site tRNA (yellow), P- (orange) and E-site (red) tRNAs and mRNA (green) are all visible [12]. **(c)** The 50S subunit of the 70S functional complex viewed from the subunit interface. The P- and E-site tRNAs are shown [12].

indicates that the structures represent a stable and, most likely, physiologically relevant state of the ribosome.

The recent structures bring a significant amount of new information about the molecular basis of ribosomal function and explain a wealth of biochemical and genetic data. Because the majority of the interactions between the ribosome and tRNA are RNA–RNA interactions, these findings provide new insights into the nature of biologically

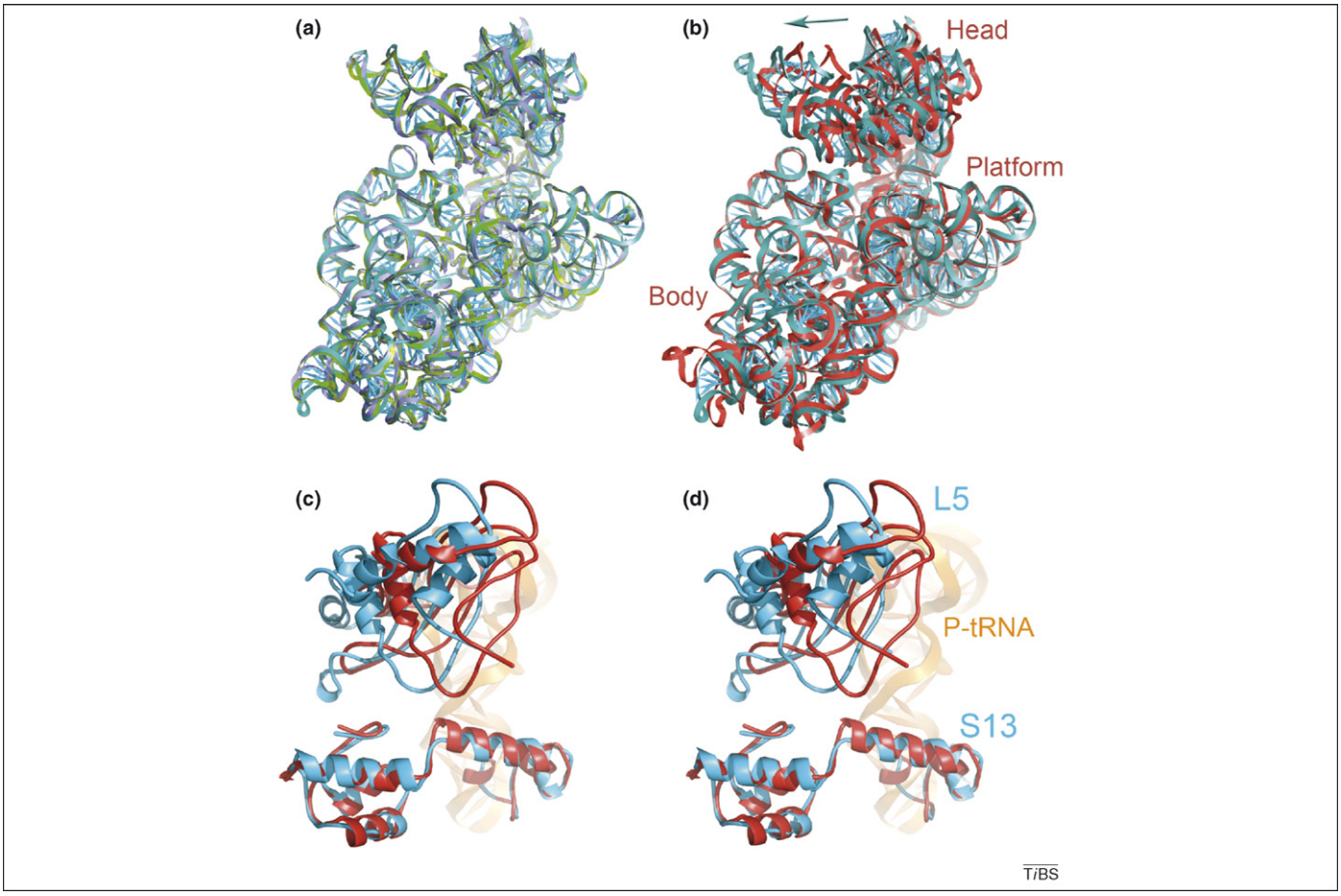

Figure 2. Conformational differences between tRNA-bound and vacant ribosomes. **(a)** Superposition of the 16S rRNA body and platform regions of the $tRNA^{fMet}$ ([12], PDB ID 2J02, cyan) and the $tRNA^{Phe}$ ([13], 2OW8, blue; [14], 2HGP, green) *T. thermophilus* 70S ribosomal complexes. Despite being crystallized in different crystal forms, all three 70S tRNA-bound complexes have similar overall conformations. 16S rRNA is shown as an example of one of the most dynamic parts of the ribosome. **(b)** By contrast, there are striking differences between the conformations of tRNA-bound *T. thermophilus* ([12], cyan) and vacant *E. coli* ([11], 2AVY, red) ribosomes. The arrow shows the direction of the 30S head movement upon tRNA binding. **(c)** Stereo view of the rearrangements that are observed in the intersubunit bridge B1b/B1c (formed by proteins S13 and L5) caused by tRNA binding. There is a noticeable shift in the position of the L5 protein relative to S13 upon tRNA binding. In the image, red represents the unoccupied state [11], and cyan represents the tRNA-bound state [12]. The position of the P-tRNA is shown (orange).

functional RNAs. The universal phylogenetic conservation of most ribosomal features involved in these interactions and the similarity between the structures of bacterial and archaeal 50S subunits [4,11–13,50] make it likely that they will turn out to be common to all ribosomes, including those of the eukaryotes.

The structures solved at 2.8 [12] and 3.7 Å [13] resolution describe functional complexes of the 70S ribosome that contain defined mRNAs with cognate $tRNA^{fMet}$ and $tRNA^{Phe}$, respectively, bound to the P site and with non-cognate tRNAs bound to the E site. In the 2.8 Å structure, the anticodon stem-loop (ASL) portion of a tRNA bound to the A site in the presence of the antibiotic paromomycin could also be resolved [12]. For the purpose of this review, these structures will be referred to as the $tRNA^{fMet}$ [12] and $tRNA^{Phe}$ [13] complexes, respectively.

The A site

The ribosomal A site is responsible for the recognition of aminoacyl-tRNA and positioning of the aminoacyl moiety for the peptidyl transferase reaction. Interactions between 16S rRNA nucleotides G530, A1492 and A1493 and the codon–anticodon helix were first observed in complexes of the isolated 30S subunit with an ASL-oligonucleotide mRNA complex [15]. These interactions have now been visualized for full-length tRNAs in the 70S ribosome complex [12], confirming the role of these universally conserved bases in the discrimination of aminoacyl-tRNA. The sharp kink in the mRNA between the A and P codons [16], which allows simultaneous codon–anticodon pairing with both codons and might be important for maintaining the translational reading frame, is now seen to be stabilized by the coordination of a magnesium ion with an mRNA backbone phosphate [12].

The acceptor end and body of the A-site tRNA (A-tRNA) are disordered in the high-resolution 70S complex [12], so our present description of their interactions with the ribosome relies on the lower-resolution 70S structures [10,14] and structures of the 50S subunit complexed with A-tRNA oligonucleotide analogs [17]. A potential disadvantage of using small model substrates is that interactions with the missing part of the tRNA might be required to form the physiologically correct structure. This is emphasized in recent studies by Schmeing *et al.* [17], who observe that lengthening their model A-site substrate by a single nucleotide results in a conformational rearrangement that positions the P-site substrate for attack by the aminoacyl-tRNA. Stacking the C74 residue of the aminoacyl-tRNA analog with the U2555 residue of the 23S rRNA leads to a slight movement of the A-loop nucleotide G2553; a greater shift of G2583, U2584 and U2585; and a 90° swing of U2506, resulting in disruption of the G2583–U2506 wobble pair. (Note, the numbering scheme of the residues here and throughout is from the *E. coli* rRNA.) Together, these displacements cause an opening near the P-site substrate, and this opening allows the peptidyl moiety and the sugar of the A76 residue of the peptidyl-tRNA to rearrange and thus expose the ester to attack from the A site. Given the differences observed between the structures of complexes containing tRNA analogs of different lengths, a conclusive description of the interactions in the A site must wait until high-resolution structures containing full-length A-site tRNAs are available.

The P site

The roles of the P site include binding the initiator tRNA (which, in bacteria, is formyl-methionyl-tRNA, or fMet-$tRNA^{fMet}$) during the initiation of protein synthesis, maintaining the correct translational reading frame and preventing loss of the nascent polypeptide chain. In both the $tRNA^{fMet}$ and $tRNA^{Phe}$ complexes described in the introduction above, the fraction of surface area buried by the ribosome and the number of interactions with the P-site tRNA (P-tRNA) exceeds that of the E-site tRNA (E-tRNA) by approximately a third, whereas the A-tRNA appears to form slightly fewer contacts than the E-tRNA (Supplementary Table 1). This is reflected in their relative binding affinities; the binding of deacylated tRNA to the P site is the strongest, whereas its affinity for the A and E sites is one to two orders of magnitude weaker [18–20].

Recent crystal structures of 70S ribosome complexes that contain full-length tRNAs [12,13] or an ASL [21] bound to the P site provide a detailed description of the numerous contacts that the ribosome makes with the tRNA and the P-site codon (Figure 3). On the small subunit, the P-site ASL is fixed by interactions with ten 16S rRNA nucleotides (which include four post-transcriptionally methylated nucleotides [22]) and the C-terminal tails of proteins S9 and S13, in addition to base pairing with its codon. The anticodon of P-site tRNA is buttressed by stacking between base m^5C1400 and the tRNA wobble base (G34), as Ofengand, Zimmermann *et al.* predicted in 1982 [23], and by packing $m^2{}_2G966$ against ribose 34. The phosphate group of mRNA P-codon nucleotide 3 is stabilized by hydrogen bonds with the 4-methylamino group of $m^4Cm1402$ and the amino group of C1403. At the junction between the P and E codons, the ribose of the third nucleotide of the E codon interacts with the 790 loop of 16S rRNA via coordination with a magnesium ion. m^3U1498 packs against the ribose–phosphate backbone of nucleotides 1 and 2 of the P codon, whereas the N1 and N2 positions of G926 are H-bonded to phosphate 1 of the P codon.

Additional stabilization of the P-site ASL comes from G1338 and A1339, which are located in the head of the small subunit and form type II and type I A-minor interactions [24] with the G–C base pairs 29:41 and 30:40 of initiator tRNA. According to mutational studies, these interactions help to differentiate between the initiator tRNA and elongator tRNAs [25,26]. A790 interacts with the opposite face of the ASL by stacking on the ribose of tRNA nucleotide 38. Together, the G1338–U1341 ridge and A790 form a 'gate' that prevents the P-site tRNA from slipping into the E site [11]. The distance between A790 and A1340 is ~15 Å; additional opening by more than 5 Å, presumably through movement of the 30S head, allows translocation to the E site. The possibility of such movement is supported by a comparison of the structures of the $tRNA^{fMet}$ or $tRNA^{Phe}$ complexes with those of vacant ribosomes [11], where the distance between A790 and A1340 is decreased by 2–3 Å.

Extensive interactions between the small subunit and tRNA in the P site contrast with those in the A site,

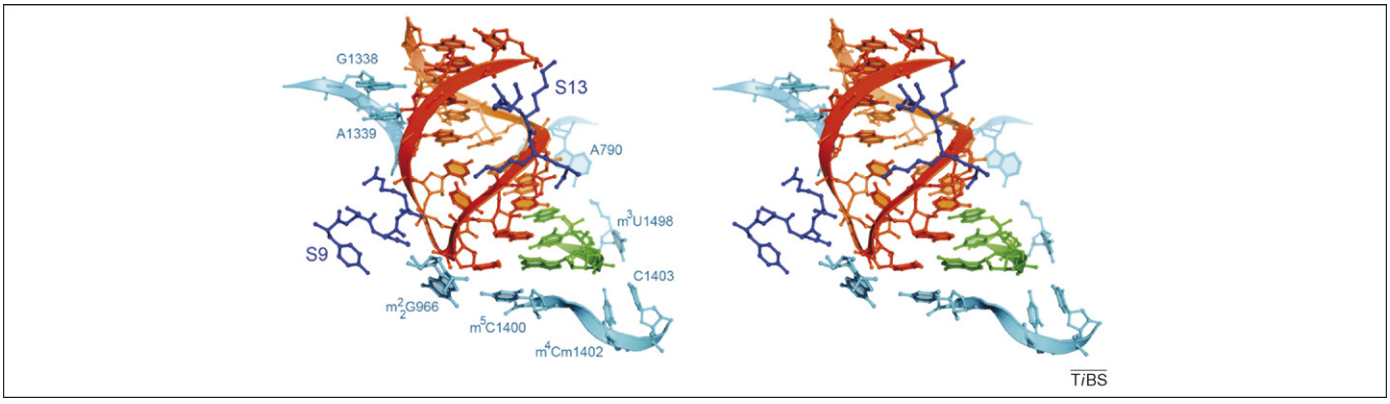

Figure 3. Interactions in the 30S P site. Stereo view showing the interactions of the ASL of initiator $tRNA^{fMet}$ (orange) and mRNA (green) with the 16S rRNA (cyan) and small-subunit proteins (blue) in the 30S subunit P site [12].

which, in keeping with its role in selecting cognate aminoacyl-tRNA, contacts the tRNA and mRNA with only four nucleotides of 16S rRNA [12]. The minimal interactions between the 30S A site and the third-position codon and anticodon nucleotides explain the prevalence of third-position wobble in the genetic code; by contrast, the absence of any direct interactions with first-position bases in the P site explains why wobble pairing with initiator tRNA is tolerated in the first position.

In the 50S P site, the minor groove of the P-tRNA D stem rests on the minor groove of helix 69 of 23S rRNA, and the elbow of the tRNA contacts an extended β-hairpin loop of protein L5. The backbone of nucleotides 2 and 3 of the acceptor stem packs against the backbone of G2255 of the P stem (helix 80) of 23S rRNA. The β-hairpin at position 82 of protein L16 comes within 10 Å of the major-groove face of the acceptor stem of P-tRNA at positions 2 and 64; its position between the 50S A and P sites suggests that L16 could interact transiently with the tRNA during translocation from the A to the P site.

The peptidyl transferase center

On the basis of biochemical and genetic studies, 23S rRNA has long been suspected to be the functional component of the peptidyl transferase center [27,28]. This was convincingly demonstrated when the high-resolution structure of the 50S subunit showed that there is no protein within 18 Å of the site of catalysis in the *Haloarcula marismortui* ribosome [4]. The overall topology of the peptidyl transferase center in the $tRNA^{fMet}$ complex is similar to that of the archaeal ribosome [17]. However, in the $tRNA^{Phe}$ complex, movement of three critical nucleotides of the catalytic site is observed [13]; this movement brings the non-canonical A2450–C2063 base pair and the catalytically important 2′-hydroxyl group of A76 of the P-site tRNA into close proximity. This raises the possibility, also suggested by mutational studies [29], that this conserved A–C pair of 23S rRNA might play a role in the peptidyl-transferase function. Given the limitations of its lower resolution, the structure of the $tRNA^{Phe}$ complex will have to be solved at a higher resolution for a conclusive description of the details of the observed changes.

In contrast to the protein-free environment of the *H. marismortui* peptidyl transferase center, the N-terminal tail of protein L27 was found to extend toward the Hoogsteen edge of A76 of the P-tRNA in the *T. thermophilus* $tRNA^{fMet}$ complex [12]. Although this apparent heterodoxy is in agreement with mutational studies showing that deletion of the L27 tail impairs peptidyl transferase function [30], it is unlikely to play a direct role in catalysis because bacterial cells survive the deletion of L27 and no counterpart to L27 is found in archaeal ribosomes [31,32]. It is more likely that L27, together with the magnesium ions that coordinate with tRNA phosphates 75 and 76, plays a role in influencing the conformation of the CCA tail of the tRNA.

The 70S E site

After peptide bond formation, the deacylated tRNA translocates from the P site to the E site. The E site is believed to provide a favorable free-energy change for movement of the deacylated tRNA out of the 50S P site [33,34]. In all of the recently solved *T. thermophilus* 70S ribosomal complexes, the E site is fully occupied by non-cognate tRNAs. The sole interaction between the E-tRNA and 16S rRNA is through a magnesium-mediated contact between tRNA phosphate 35 and 16S rRNA phosphate 1340, explaining the absence of a base-specific footprint for tRNA in the 30S E site [35,36]. By contrast, the ASL of E-tRNA interacts extensively with basic side chains of proteins S7 and S11. No codon–anticodon pairing has been observed in these structures; however, a definitive answer is impossible without elucidation of the structure of an elongation complex containing a cognate E-tRNA.

In the 50S subunit, numerous interactions with 23S rRNA fix the E-tRNA in position (Figure 4). The L1 stalk (23S rRNA helices 76–78) and protein L1 contact the elbow of the tRNA (Figures 4a,b). According to the structure of the $tRNA^{Phe}$ complex, the contact involves stacking the universally conserved G19–C56 base pair of tRNA on the tertiary G2112–A2169 base pair of 23S rRNA. This interaction accounts for the protection of G2112 and A2169 from chemical probes by E-tRNA [37] and is in agreement with the tertiary G2112–A2169 base pair observed in the crystal structure of an RNA fragment derived from the L1 stalk of 23S rRNA [38]. By contrast, the structure of $tRNA^{fMet}$ complex shows stacking of the C19–C56 base pair of the E-tRNA on a tertiary pair formed between G2112 and G2168, whereas A2169 is paired with U2113. The high temperature factors reported for this region of the

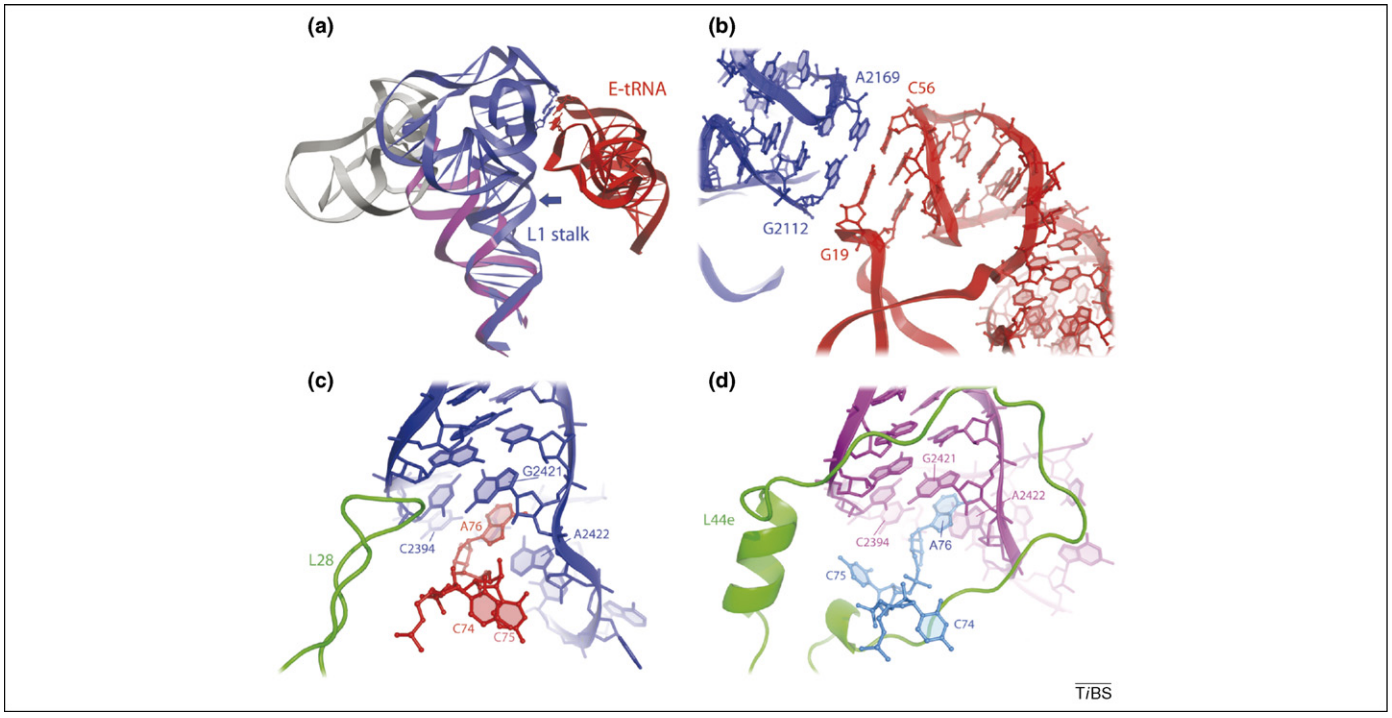

Figure 4. E-tRNA interactions. **(a)** Interaction of the elbow of E-tRNA (red) with 23S rRNA (blue) in the L1 stalk region [13], showing the large-scale displacement of the stalk relative to its position (represented by magenta for observed and grey for modeled rRNA) in the vacant ribosome [11], induced by tRNA binding. The blue arrow indicates the extreme compression of the major groove of helix 76 of 23S rRNA that accompanies this movement. **(b)** Stacking of the G19–C56 tertiary base pair of the E-tRNA on the G2112–A2169 tertiary pair of 23S rRNA. **(c)** Comparison of the conformations and binding of the CCA tail of tRNA to the E site of the *T. thermophilus* 70S complex [13] and **(d)** a CCA-containing RNA hairpin designed to mimic the tail of a tRNA bound to the *H. marismortui* 50S E site [42].

$tRNA^{fMet}$ complex suggest that this discrepancy is due to poor order in this region of the structure. The rest of the interactions with the E-tRNA elbow are made by two β-hairpin loops of protein L1, which contact the T stem and T loop.

The acceptor stem of the E-tRNA is involved in intimate backbone–backbone interactions at nucleotides 70–71 with the minor groove of helix 68 of 23S rRNA. Experiments in which methylation of ribose 71 was found to impair the ability of the P-tRNA to move into the P/E hybrid state have demonstrated the importance of this interaction [39]. The backbone of the tRNA acceptor stem at nucleotides 73 and 74 interacts with the extended β hairpin of protein L28. As visualized in the $tRNA^{fMet}$ complex, L33 hydrogen bonds with phosphate 67 via the side chain of Arg28. Although L33 has been crosslinked to the 3′-terminal adenosine of E-tRNA [40], there appears to be no direct interaction between L33 and A76. Because L33 is also within 15 Å of the D loop of P-tRNA, it could transiently interact with the tRNA as it translocates from the P to the E site.

Crucial to E-tRNA binding is its 3′-terminal adenosine, which must be deacylated and unmodified [39,41]. The recent crystal structures show that A76 is recognized and fixed in position by extensive stacking and hydrogen-bonding interactions with 23S rRNA. As first seen in the complex between the isolated *H. marismortui* 50S subunit and a CCA-containing RNA hairpin analog of E-tRNA [42], A76 intercalates between bases G2421 and A2422 (Figures 4c,d). The 3′ adenosine hydrogen bonds to phosphate 2422 of 23S rRNA and to Asn33 of protein L35 [12]. A magnesium ion that is bound between phosphates 2431 and 2432 of 23S rRNA might interact with the 3′-hydroxyl of A76 and help to stabilize the network of E-site interactions between 23S rRNA and the deacylated A76. The 2′ hydroxyl of ribose 76 is hydrogen bonded to C2394, as also seen in the aforementioned 50S model complex [42], helping to explain the specificity of the E site for deacylated tRNA [41], protection of C2394 by E-tRNA [37] and destabilization of E-site binding by methylation of the 2′ hydroxyl [43] or by mutation of C2394 to G [44].

The path of the 3′ CCA tail of the E-tRNA, however, is strikingly different from that observed in the 50S complex (Figures 4c,d). In the 70S complexes, C74 and C75 are stacked continuously with nucleotide 73 and the acceptor stem of the tRNA, whereas in the 50S complex, C75 is flipped out on the opposite site of the backbone. These variations are probably due to phylogenetic differences between the source species for the 70S and 50S complexes; in the 70S complex, a flipped C75 would clash with protein L28, which in the archaeal ribosome is replaced by L44e, a protein of unrelated sequence or fold. An alternative interpretation of the observed differences between the 50S and 70S E-site interactions is that the 50S complex more closely resembles the state of the acceptor stem in the P/E hybrid state than in the E/E state, as suggested by Schmeing *et al.* [42].

mRNA-ribosome interactions

During the initiation of protein synthesis in bacteria and archaea, selection of the mRNA start site is strongly influenced by base-pairing interactions between the Shine-Dalgarno (SD) sequence upstream from the start codon and the anti-SD sequence in the 3′ tail of 16S rRNA

[45]. Recently, the structures of several ribosomal complexes containing different mRNA constructs have been solved, at resolutions of 3.3 Å [46] and 4.5–5.5 Å [14], in an effort to understand the structural interactions that position the SD helix and the transition between the initiation and elongation states of mRNA. Interactions between the 30S ribosomal subunit and and an SD-helix analog [46] suggest that the formation of the SD helix in the cleft between the platform and the head of the small subunit might contribute to the stabilization of the small subunit in a state optimal for interaction with the initiator $tRNA^{fMet}$. So that a 70S initiation complex could be modeled, ribosomes were co-crystallized with initiator $tRNA^{fMet}$ and an mRNA fragment containing a four-nucleotide aligned spacer between the SD sequence and the AUG start codon [47]. In this state, the SD helix is positioned next to the N terminus of protein S18. A post-initiation complex was formed with elongator $tRNA^{Phe}$ bound at all three ribosomal binding sites and an mRNA containing a 6-nucleotide spacer between the P codon and SD sequence. In this structure, the spacer relaxes, leading to a significant displacement of the SD helix by up to 18 Å and causing it to bend away from protein S18 toward S2. In an elongation complex containing an mRNA fragment lacking an SD sequence, electron density for the mRNA upstream from the E codon is very weak, suggesting that the upstream region of the mRNA is flexible and not involved in specific interactions with the ribosome. Based on these findings, Yusupova *et al.* propose a stepwise series of interactions between the ribosome and the SD region of mRNA during initiation. These interactions involve (i) formation of the SD helix; (ii) its binding near protein S2; (iii) rearrangement toward protein S18 upon docking of the initiation codon into the ribosomal P site; (iv) relaxation of the mRNA after the first step of translocation, allowing displacement of the SD helix toward protein S2; and (v) continuous movement of mRNA in the 3′-to-5′ direction and eventual melting of the SD duplex as translocation proceeds. It should be noted, however, that the initiation-like complex used in this study differs in detail from a true initiation complex; for example, the E site of the initiation-like complex is occupied by tRNA. Thus, further studies will be required to clarify the significance of repositioning the SD helix.

Ribosome and tRNA dynamics

Both the ribosome and its bound tRNAs undergo conformational changes as a result of their mutual interactions. Large-scale ribosomal rearrangements that result from the ribosome's interactions with tRNA include the rotation of the the small subunit's head (Figure 2b) and the movement of the L1 stalk of the 50S subunit to interact with the E-tRNA (Figure 4a) [3,11–13,48]. Interestingly, the pivot point for movement can be localized to rRNA helices in the vicinity of conserved G–U base pairs in both cases. Because the presence of G–U pairs has been observed to increase the flexibility of RNA helices [49,50], their occurrence at pivot points can facilitate ribosomal movements as well as constrain their geometry. Upon tRNA binding, the small subunit closes by pivoting in the neck region within 16S rRNA helix 28 and thus causes the head to rotate by up to 12° (Figure 2b). Partial closure of the small subunit is also observed in the presence of an ASL fragment of P-tRNA [21]. In the 50S subunit, the head of the L1 stalk (23S rRNA helices 76–78 and protein L1) contacts the elbow of E-tRNA. To make contact, the stalk moves by more than 30 Å relative to the structures of the vacant 70S ribosome [11] or the isolated 50S subunit [51]; the hinge point is between nucleotides 2187–2193 and 2096–2102 of helix 76 (Figure 4a). Reversal of this movement of the L1 stalk would be required to allow release of the deacylated tRNA from the ribosome.

Several smaller-scale rearrangements, including changes in intersubunit contacts, occur upon tRNA binding.

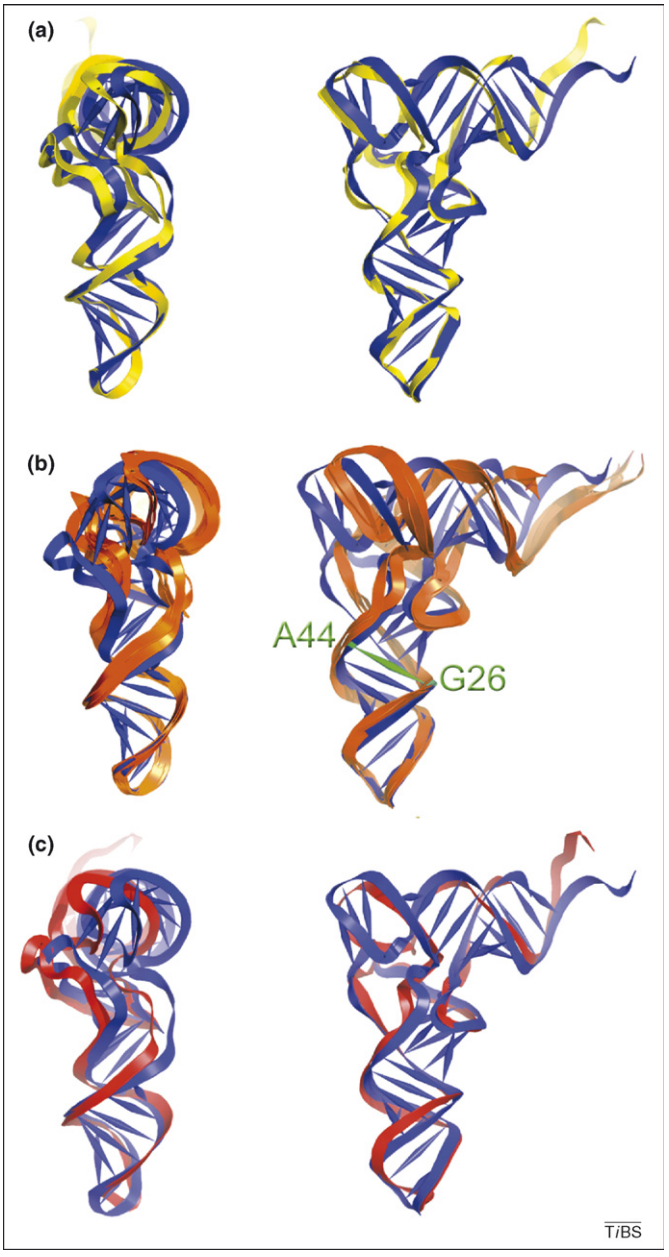

Figure 5. Distortion of tRNA structure by the ribosome. The structure of free $tRNA^{Phe}$ ([52], blue) is superimposed with those of **(a)** A-site $tRNA^{Phe}$ ([14], yellow), **(b)** P-$tRNA^{fMet}$ of initiation-like and P-$tRNA^{Phe}$ of elongation-like complexes ([12–14], orange) and **(c)** E-tRNA of the elongation-like ribosomal complex ([13], red). In each case, the right-hand image is obtained by rotation of the left-hand image 90° around its vertical axis. The position of the G26–A44 purine–purine base pair is shown where kinking of the tRNA occurs in all three ribosomal binding sites.

Protein L5 moves more than 3 Å away from the P site to accommodate the tRNA; it slides along the α-helix of protein S13 by more than 4 Å and rearranges the bridge B1b/B1c relative to its structure in the vacant ribosome (Figure 2c). In the $tRNA^{Phe}$ complex, an additional bridge contact is observed between S13 and the tip of the A-site finger (helix 38) of 23S rRNA. This part of helix 38 is disordered in the vacant ribosome structure, suggesting that its contact with S13 is formed upon binding tRNA. Another new bridge is formed in response to the binding of A-site tRNA [12]. A1913 in the loop of 23S rRNA helix 69 protrudes into a pocket formed by the penultimate stem (h44) of 16S rRNA and the A-site tRNA. This bridge appears to be stabilized by hydrogen bonding between A1913 and the ribose of tRNA nucleotide 37 and interactions with two magnesium ions. In both the vacant and $tRNA^{Phe}$ ribosomes [11,13], where no A-tRNA is found, A1913 is instead inserted into the minor groove of helix 44 of 16S rRNA.

tRNA also undergoes conformational changes upon interaction with the ribosome, as first observed in cryo-EM reconstructions of ribosomes bound with the ternary complex EF-Tu·GDP·kirromycin·tRNA, in which the anticodon–stem loop of the A/T-state tRNA is kinked by more than 30° [2]. In the 5.5 Å X-ray structure [14], the body of the A-tRNA rotates by ~10° relative to the ASL, toward the P site (Figure 5a). As in the A/T state [2], the hinge point lies at the G26–A44 purine–purine base pair. Distortion of the P-tRNA is more pronounced: the body is bent toward the large subunit by ~10° (Figure 5b). In addition, partial unwinding of the D stem relative to the ASL leads to a rotation of the body of the P-tRNA by ~10° around the axis of the anticodon arm, orienting the body slightly toward the A site (Figure 5b). Kinking of the E-tRNA is very similar to that of the A-tRNA (Figure 5c). Thus, tRNA appears to favor two distinguishable conformations when bound to the three classical binding sites of the ribosome, both of which differ from the structure of isolated tRNA [52]. If the conformation of the P-tRNA is the least energetically favorable one, the strong binding affinity of tRNA for the P site (discussed above) might be due in part to the necessity of preserving its distorted conformation. After peptide-bond formation, this conformational-strain energy could contribute to the driving force for translocation to the 50S E site.

Conclusions

New X-ray structures of 70S ribosome functional complexes at improved resolution add significantly to our detailed understanding of the molecular basis of the interactions between the ribosome and its mRNA and tRNAs. Moreover, most of these results will be immediately applicable to the largely undescribed structure of the 80S ribosome because of the extraordinary phylogenetic conservation of many of the functional features of 70S ribosomes. Although of fundamental biological importance, the ability of ribosomes to bind mRNA and tRNA is itself unremarkable; nor is the ribosome's catalytic activity impressive when compared to those of conventional acyl transferases. What is remarkable, however, is that in the ribosome these functions are carried out largely by RNA, not protein, and this is undoubtedly the palimpsest of the origins of these mechanisms in early molecular evolution. Perhaps most impressive is the ability of the ribosome, together with elongation factor EF-G, to translocate mRNA and tRNAs over very large molecular distances with high speed and accuracy while maintaining the correct translational reading frame. Also striking is the speed and accuracy with which aminoacyl-tRNAs are selected by the ribosome, in this case in conjunction with elongation factor EF-Tu. Yet our understanding of both of these fundamental steps of protein synthesis is only rudimentary, despite decades of (often ingenious and elegant) experimentation. This is at least partly due to the lack of high-resolution structural descriptions of ribosomal complexes relevant to these basic mechanisms. Thus, the future challenge for ribosome crystallography will be to solve the ribosome in all of its structural states and, ultimately, to provide an atomic-resolution description of its interactions, catalysis and dynamics through the whole complicated process of protein synthesis.

Acknowledgements

We apologize to our many colleagues whose studies have not been mentioned because of space limitations. We thank Dmitri Ermolenko, Laura Lancaster and Clint Spiegel for helpful discussions; Martin Laurberg and Sergei Trakhanov for their contributions to structure determination; and Carl Gorringe for assistance in figure preparation. This work was supported by grants (to H.F.N.) from the National Institutes of Health and the National Science Foundation.

Supplementary data

Supplementary data associated with this article can be found, in the online version, at doi:10.1016/j.tibs.2007.08.002.

References

1 Agrawal, R.K. *et al.* (1996) Direct visualization of A-, P-, and E-site transfer RNAs in the *Escherichia coli* ribosomes. *Science* 271, 1000–1002
2 Valle, M. *et al.* (2002) Cryo-EM reveals an active role for aminoacyl-tRNA in the accommodation process. *EMBO J.* 21, 3557–3567
3 Gao, H. *et al.* (2003) Study of the structural dynamics of the *E. coli* 70S ribosome using real-space refinement. *Cell* 113, 789–801
4 Ban, N. *et al.* (2000) The complete atomic structure of the large ribosomal subunit at 2.4 Å resolution. *Science* 289, 905–920
5 Schluenzen, F. *et al.* (2000) Structure of functionally activated small ribosomal subunit at 3.3 angstroms resolution. *Cell* 102, 615–623
6 Wimberly, B.T. *et al.* (2000) Structure of the 30S ribosomal subunit. *Nature* 407, 327–339
7 Muth, G.W. *et al.* (2000) A single adenosine with a neutral pKa in the ribosomal peptidyl transferase center. *Science* 289, 947–950
8 Ogle, J.M. *et al.* (2003) Insights into the decoding mechanism from recent ribosome structures. *Trends Biochem. Sci.* 28, 259–266
9 Cate, J.H. *et al.* (1999) X-ray crystal structures of 70S ribosome functional complexes. *Science* 285, 2095–2104
10 Yusupov, M. *et al.* (2001) Crystal structure of the ribosome at 5.5 Å resolution. *Science* 292, 883–896
11 Schuwirth, B.S. *et al.* (2005) Structures of the bacterial ribosome at 3.5 Å resolution. *Science* 310, 827–834
12 Selmer, M. *et al.* (2006) Structure of the 70S ribosome complexed with mRNA and tRNA. *Science* 313, 1935–1942
13 Korostelev, A. *et al.* (2006) Crystal structure of a 70S ribosome-tRNA complex reveals functional interactions and rearrangements. *Cell* 126, 1065–1077
14 Yusupova, G. *et al.* (2006) Structural basis for messenger RNA movement on the ribosome. *Nature* 444, 391–394
15 Ogle, J.M. *et al.* (2001) Recognition of cognate transfer RNA by the 30S ribosomal subunit. *Science* 292, 897–902

16 Yusupova, G.Z. *et al.* (2001) The path of messenger RNA through the ribosome. *Cell* 106, 233–241
17 Schmeing, T.M. *et al.* (2005) An induced-fit mechanism to promote peptide bond formation and exclude hydrolysis of peptidyl-tRNA. *Nature* 438, 520–524
18 Holschuh, K. and Gassen, H.G. (1982) Mechanism of translocation. Binding equilibria between the ribosome, mRNA analogues, and cognate tRNAs. *J. Biol. Chem.* 257, 1987–1992
19 Lill, R. *et al.* (1986) Affinities of tRNA binding sites of ribosomes from *Escherichia coli*. *Biochemistry* 25, 3245–3255
20 Schilling-Bartetzko, S. *et al.* (1992) Kinetic and thermodynamic parameters for tRNA binding to the ribosome and for the translocation reaction. *J. Biol. Chem.* 267, 4703–4712
21 Berk, V. *et al.* (2006) Structural basis for mRNA and tRNA positioning on the ribosome. *Proc. Natl. Acad. Sci. U. S. A.* 103, 15830–15834
22 Guymon, R. *et al.* (2006) Influence of phylogeny on posttranscriptional modification of rRNA in thermophilic prokaryotes: the complete modification map of 16S rRNA of *Thermus thermophilus*. *Biochemistry* 45, 4888–4899
23 Prince, J.B. *et al.* (1982) Covalent crosslinking of tRNA1Val to 16S RNA at the ribosomal P site: identification of crosslinked residues. *Proc. Natl. Acad. Sci. U. S. A.* 79, 5450–5454
24 Nissen, P. *et al.* (2001) RNA tertiary interaction in the large ribosomal subunit: the A-minor motif. *Proc. Natl. Acad. Sci. USA* 98, 4899–4903
25 Lancaster, L. and Noller, H.F. (2005) Involvement of 16S rRNA nucleotides G1338 and A1339 in discrimination of initiator tRNA. *Mol. Cell* 20, 623–632
26 Abdi, N.M. and Fredrick, K. (2005) Contribution of 16S rRNA nucleotides forming the 30S subunit A and P sites to translation in *Escherichia coli*. *RNA* 11, 1624–1632
27 Green, R. and Noller, H.F. (1997) Ribosomes and translation. *Annu. Rev. Biochem.* 66, 679–716
28 Noller, H.F. *et al.* (1992) Unusual resistance of peptidyl transferase to protein extraction procedures. *Science* 256, 1416–1419
29 Hesslein, A.E. *et al.* (2004) Exploration of the conserved A+C wobble pair within the ribosomal peptidyl transferase center using affinity purified mutant ribosomes. *Nucleic Acids Res.* 32, 3760–3770
30 Maguire, B.A. *et al.* (2005) A protein component at the heart of an RNA machine: the importance of protein l27 for the function of the bacterial ribosome. *Mol. Cell* 20, 427–435
31 Dabbs, E.R. (1991) Mutants lacking individual ribosomal proteins as a tool to investigate ribosomal properties. *Biochimie* 73, 639–645
32 Wower, I.K. *et al.* (1998) Ribosomal protein L27 participates in both 50 S subunit assembly and the peptidyl transferase reaction. *J. Biol. Chem.* 273, 19847–19852
33 Lill, R. *et al.* (1989) Binding of the 3′ terminus of tRNA to 23S rRNA in the ribosomal exit site actively promotes translocation. *EMBO J.* 8, 3933–3938
34 Moazed, D. and Noller, H.F. (1989) Intermediate states in the movement of transfer RNA in the ribosome. *Nature* 342, 142–148
35 Moazed, D. and Noller, H.F. (1986) Transfer RNA shields specific nucleotides in 16S ribosomal RNA from attack by chemical probes. *Cell* 47, 985–994
36 Moazed, D. and Noller, H.F. (1990) Binding of tRNA to the ribosomal A and P sites protects two distinct sets of nucleotides in 16S rRNA. *J. Mol. Biol.* 211, 135–145
37 Moazed, D. and Noller, H.F. (1989) Interaction of tRNA with 23S rRNA in the ribosomal A, P, and E sites. *Cell* 57, 585–597
38 Nikulin, A. *et al.* (2003) Structure of the L1 protuberance in the ribosome. *Nat. Struct. Biol.* 10, 104–108
39 Feinberg, J. and Joseph, S. (2001) Identification of molecular interactions between P site tRNA and the ribosome essential for tanslocation. *Proc. Natl. Acad. Sci. U. S. A.* 98, 11120–11125
40 Kirillov, S.V. *et al.* (2002) Transit of tRNA through the *Escherichia coli* ribosome: cross-linking of the 3′ end of tRNA to ribosomal proteins at the P and E sites. *FEBS Lett.* 514, 60–66
41 Lill, R. *et al.* (1988) Specific recognition of the 3′-terminal adenosine of tRNAPhe in the exit site of *Escherichia coli* ribosomes. *J. Mol. Biol.* 203, 699–705
42 Schmeing, T.M. *et al.* (2003) Structures of deacylated tRNA mimics bound to the E site of the large ribosomal subunit. *RNA* 9, 1345–1352
43 Bocchetta, M. *et al.* (2001) Interactions between 23S rRNA and tRNA in the ribosomal E site. *RNA* 7, 54–63
44 Sergiev, P.V. *et al.* (2005) Function of the ribosomal E-site: a mutagenesis study. *Nucleic Acids Res.* 33, 6048–6056
45 Gold, L. (1988) Posttranscriptional regulatory mechanisms in *Escherichia coli*. *Annu. Rev. Biochem.* 57, 199–233
46 Kaminishi, T. *et al.* (2007) A snapshot of the 30S ribosomal subunit capturing mRNA via the Shine-Dalgarno interaction. *Structure* 15, 289–297
47 Chen, H. *et al.* (1994) Determination of the optimal aligned spacing between the Shine-Dalgarno sequence and the translation initiation codon of *Escherichia coli* mRNAs. *Nucleic Acids Res.* 22, 4953–4957
48 Valle, M. *et al.* (2003) Locking and unlocking of ribosomal motions. *Cell* 114, 123–134
49 Chang, K.Y. *et al.* (1999) Correlation of deformability at a tRNA recognition site and aminoacylation specificity. *Proc. Natl. Acad. Sci. U. S. A.* 96, 11764–11769
50 Ramos, A. and Varani, G. (1997) Structure of the acceptor stem of *Escherichia coli* tRNA Ala: role of the G3.U70 base pair in synthetase recognition. *Nucleic Acids Res.* 25, 2083–2090
51 Harms, J. *et al.* (2001) High resolution structure of the large ribosomal subunit from a mesophilic eubacterium. *Cell* 107, 679–688
52 Jovine, L. *et al.* (2000) The crystal structure of yeast phenylalanine tRNA at 2.0 Å resolution: cleavage by Mg(2+) in 15-year old crystals. *J. Mol. Biol.* 301, 401–414